

Regular paper

Erythrocyte nitric oxide transport reduced by a submembrane cytoskeletal barrier

Tae H. Han, James C. Liao*

Department of Chemical Engineering, 5531 Boelter Hall, University of California, Los Angeles, CA 90095-1592, USA

Received 11 October 2004; received in revised form 4 January 2005; accepted 18 January 2005

Available online 23 February 2005

Abstract

Encapsulation of hemoglobin (Hb) within red blood cells (RBCs) preserves nitric oxide (NO) bioactivity. With encapsulation, millimolar concentrations of Hb quench only a fraction of NO bioactivity, whereas mere micromolar concentrations of cell-free Hb completely quench NO bioactivity. A submembrane cytoskeletal barrier has been hypothesized to account for the lowered quenching of NO bioactivity. In order to substantiate this hypothesis, here, the underlying submembrane cytoskeletal barrier was physically reduced and the rate of NO entry into the modified RBC measured. The submembrane cytoskeletal barrier of normal and depleted RBCs was characterized using atomic force microscopy and the lipid to protein ratio measured. The reduction in the submembrane cytoskeletal barrier resulted in an increase in the rate of NO entry. We suggest that the underlying submembrane cytoskeleton may be a key component of RBC mediated regulation of NO bioavailability.

© 2005 Elsevier B.V. All rights reserved.

Keywords: Nitric oxide; Erythrocyte; Red blood cell; Cytoskeleton; Membrane

1. Introduction

Nitric oxide (NO) is endogenously produced in many cells for a variety of functions. In the vasculature, NO is produced by endothelial cells in order to regulate blood flow. Endothelium derived NO freely diffuses into adjacent smooth muscle cells to activate soluble guanylyl cyclase. The activation of guanylyl cyclase initiates a cascade of reactions that results in vasodilation [1–4]. Nitric oxide also freely diffuses into the lumen, where it is scavenged by hemoglobin (Hb), which exists at millimolar concentrations in red blood cells (RBCs) [5,6].

Oxyhemoglobin (oxyHb) converts NO to nitrate, whereas deoxygenated hemoglobin binds NO to form iron-nitrosylhemoglobin. In the presence of excess Hb, the half-life of NO is on the order of microseconds ($k \sim 10^7 \text{ M}^{-1} \text{ s}^{-1}$) [5,6]. As NO is produced adjacent to Hb-rich blood (10 mM) and Hb rapidly deactivates NO bioactivity [5–12], how NO escapes to activate soluble guanylyl cyclase is a question that has received considerable attention [8,13–15]. In partial resolution to this question, the enclosure of Hb within RBCs [15,16] has been proposed to be the primary mode by which NO bioactivity is preserved.

Without RBC enclosure, mere micromolar concentrations of cell-free oxyHb have been shown to cause vasoconstriction [15,17] and the release of Hb from RBCs has been linked to the painful crisis episodes experienced by sickle cell patients [12]. The enclosure of Hb within RBCs alleviates vasoconstriction through (i) the creation of a RBC-free zone adjacent to the vessel wall from hydrodynamic forces [15], (ii) high extracellular diffusional

Abbreviations: NO, nitric oxide; RBCs, red blood cells; Hb, hemoglobin; oxyHb, oxyhemoglobin; metHb, methemoglobin; Sper/NO, spermine NON-Oate; AFM, atomic force microscopy; 5P8, 5 mM phosphate at pH 8.0

* Corresponding author. Tel.: +1 310 825 1656; fax: +1 310 206 4107.

E-mail address: liao@ucla.edu (J.C. Liao).

resistance from the fluid bulk to the surface of the RBC [16], and (iii) the presence of an intrinsic barrier composed of the RBC submembrane cytoskeletal protein that reduces the entry of NO into the RBC [18,19]. Although each barrier may be important under different conditions, it is the underlying protein barrier that is always present to preserve NO bioactivity [18,19]. Moreover, RBC chemical modifications using Band 3 crosslinkers, sodium azide, phenylhydrazine, or nitric oxide, itself, have been suggested to alter the submembrane barrier and demonstrated to alter the NO consumption rate [19,20]. These changes in the NO consumption rate directly led to corresponding changes in the vessel diameter of isolated coronary arterioles [19,20]. Thus, it was suggested, based on these chemical modifications, that the submembrane cytoskeleton may be a barrier to NO entry and accounts for the preservation of NO bioavailability.

If the RBC submembrane cytoskeleton is the barrier that reduces NO entry, the physical reduction of the submembrane cytoskeleton should increase the rate that NO is consumed by the RBC. By forming white ghosts, with extensive washing to remove a portion of the submembrane cytoskeleton, and resealing with Hb, here we demonstrate that the NO uptake rate was increased. In addition, the submembrane cytoskeleton of both white and pink ghosts was imaged in their native state using atomic force microscopy (AFM). In pink ghosts, where the submembrane cytoskeleton was preserved, the NO consumption rate was not altered.

2. Materials and methods

2.1. Chemicals

The NO donor, Spermine NONOate (Sp/NO), *N*-[4-[1-(3-aminopropyl)-2-hydroxy-2-nitrosohydrazino]butyl]-1,3-propanediamine, was purchased from Alexis L.L.C. (San

Diego, CA). Sodium chloride, sodium hydroxide, and hydrochloric acid were purchased from Fisher Scientific (Tustin, CA). All other chemicals were purchased from Sigma (St. Louis, MO).

2.2. Preparation of red blood cells

Bovine blood was collected in anticoagulant citrate dextrose (15%). The plasma and buffy coat were removed following centrifugation at $800\times g$ for 10 min. The cells were resuspended in a 40 mM HEPES buffer containing 125 mM NaCl and 5 mM glucose (pH 7.4). Red blood cells were isolated from white cells by filtration through a mixture of α cellulose and microcrystalline cellulose. Red blood cells were washed again to remove any residual plasma proteins.

2.3. Preparation of oxyhemoglobin

Isolated RBCs were concentrated by incubation in a hypertonic 40 mM HEPES buffer containing 275 mM NaCl and 5 mM glucose (pH 7.4). The initial hematocrit was adjusted to 15%. The RBC suspension was then centrifuged at $800\times g$ for 20 min. All the supernatant was aspirated and the RBCs were lysed by freezing at $-80\text{ }^{\circ}\text{C}$. The lysate was centrifuged at $22,000\times g$, $4\text{ }^{\circ}\text{C}$ for 30 min and the supernatant collected (50% of the sample volume). The pellet, which contained lysed RBC membranes fragments and associated submembrane proteins, was discarded. The supernatant was centrifuged again for 30 min and the resultant supernatant collected (25% of the total sample volume). All solutions for preparing proteins were maintained at $4\text{ }^{\circ}\text{C}$.

2.4. Preparation of resealed white and pink ghosts

Resealed ghosts were prepared following the methods of Steck and Kant [21] with some modification (Fig. 1).

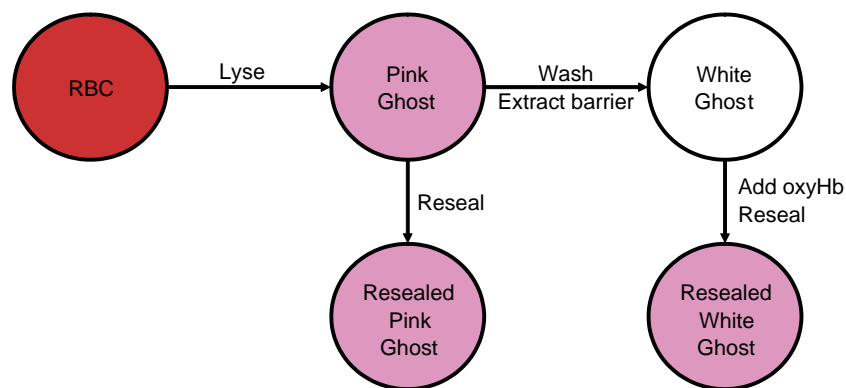


Fig. 1. Starting from isolated RBCs, pink ghosts were first prepared by lysis with 5P8 buffer. White ghosts were then prepared by a cycles of centrifugation and washing until all residual Hb was removed. Resealed pink ghosts were prepared by adding salt and incubating at $37\text{ }^{\circ}\text{C}$ for 1 h. Resealed white ghosts were prepared by first incubating the white ghosts with concentrated Hb solution on ice. After 30 min, a 5 M salt solution was added to the sample until the solution became isotonic. The sample was then incubated at $37\text{ }^{\circ}\text{C}$ for 1 h.

Briefly, 25 mL of 5 mM phosphate buffer at pH 8.0 (5P8) at 4 °C was added to 4 mL of a 50% hematocrit RBC suspension. The sample was left on ice for 5 min then centrifuged at $22,000\times g$, 4 °C for 40 min. The pellet was washed, resuspended, and centrifuged four times using 20 mL of 5P8 at $22,000\times g$, 4 °C for 20 min. The RBC submembrane pellet (white submembrane) was incubated on ice for 30 min in various concentrations of oxyHb. A 5 M NaCl solution was used to adjust the osmolality to 290 mosM/kg. The ghost submembrane was sealed by incubation in concentrated oxyHb solutions (20–30 mM) at 37 °C for 1 h. With this procedure, the maximum concentration of resealed intracellular oxyHb achieved was 1000 μM . The sealed ghosts were centrifuged at $800\times g$ for 20 min and then equilibrated with HEPES buffer. Pink ghosts were prepared by lysis of RBCs in 5P8 to the desired intracellular Hb concentration with no washing. The intracellular Hb concentration was adjusted by changing the lysis buffer to RBC ratio. Pink ghosts were resealed with a method similar to resealed white ghosts.

2.5. The competition assay for measuring the nitric oxide uptake rate by red blood cells

This procedure has been described previously [22]. A detailed description of the procedure along with the computer program for calculating the kinetic coefficient is available (<http://www.seas.ucla.edu/~liaoj>). Briefly, the competition assay measures the NO uptake rate of RBCs by allowing extracellular oxyHb to compete with RBCs in the same solution for a limited amount of NO released homogeneously by Sp/NO, a slow releasing NO donor. In a separate sample, the total amount of NO released by Sp/NO was measured by the formation of metHb in the extracellular space from the oxyHb reaction with NO. The difference in total NO released and NO consumed by extracellular oxyHb in the RBC suspension was the NO consumed by the RBC. No export of oxidizing species was detected by incubating resealed ghosts with only oxyHb in the extracellular space. No export of reducing species was detected by incubating RBCs or resealed ghosts with methemoglobin (metHb) in the extracellular space. Under these experimental conditions, neither S-nitrosated Hb nor iron-nitrosyl Hb were detected using an independent ozone-based chemiluminescence method [23]. The rate constant (k_{RBC} , or k'_{RBC}) for NO consumption by RBC was defined in the following equation

$$V_{\text{RBC}} = k_{\text{RBC}}[\text{rbCHb}][\text{NO}] = k'_{\text{RBC}}[\text{RBC}][\text{NO}]$$

where V_{RBC} is the rate of NO consumption by RBCs, $[\text{rbCHb}]$, and $[\text{NO}]$ are the concentrations of total RBC heme and NO, respectively, based on the total volume as if Hb was not enclosed by the RBC submembrane. The first definition allows the comparison between k_{RBC} with k_{Hb} (rate constant for the reaction between NO and free

oxyHb) on the same homogeneous basis. To determine the NO consumption on a per RBC basis, we used the second definition in the above equation, where $[\text{RBC}]$ is the number of RBC per unit volume. The RBC cell density was $3.0\times 10^6/\mu\text{L}$ for 15% hematocrit of bovine RBCs. For resealed ghosts, k'_{RBC} is a better definition for comparison because it is insensitive to the intracellular Hb concentration.

2.6. Measurement of the protein to lipid ratio

The protein content of each sample was measured with a commercial kit (Bio-Rad DC Protein Quantification Assay). Phospholipid content was measured using the interaction of phosphomolybdenum and malachite green as previously described [24]. Briefly, total lipids were extracted using a methanol, chloroform, water mixture in a 1:1:1 final ratio to isolate lipids. Lipids were transferred to clean glass tubes and the solvent evaporated. Lipids were then reacted with 70% perchloric acid at 180 °C for 30 min. After cooling for 20 min, a solution of 0.24% malachite green, 0.85% ammonium molybdenum, and 0.04% Tween-20 (all final concentrations) was added. After agitation, the absorbance of each sample was measured at 660 nm and compared to a phosphate calibration curve to determine phospholipid content.

2.7. Atomic force microscopy measurement of the submembrane cytoskeleton

Ghosts were placed on silane coated mica lysed with hypotonic 5 mM phosphate buffer (pH 7.2). Freshly cleaved mica slides were prepared by adhering strips of tape to opposite sides of a mica book, and then pulling the strips of tape apart. These freshly cleaved mica slides were then stored in a small enclosed chamber (<100 mL) with 0.2 mL of silane overnight. Mica slides were rinsed with water filtered through a Milli-Q filter system (Millipore) and air dried. Mica slides were used within a day.

Atomic force microscopy (AFM) measurements were carried out on a Digital Instruments Nanoscope IV Bioscope (Veeco Metrology, Santa Barbara, CA). Oxide sharpened triangular silicon nitride tips (Olympus OTR4 SiN probes, Veeco Metrology, Santa Barbara, CA) with a tip size of less than 10 nm were used (0.08 N/m spring constant). All measurements were made under isotonic 5 mM phosphate buffer and the system was allowed to thermally equilibrate for at least 1 h. In order to obtain the highest resolution images possible we paid special attention to sources of noise (acoustic, thermal, electrical) inherent in many experimental systems. The AFM was placed on a vibration isolation air table, which was housed inside an acoustic isolation chamber that also shields out electrical noise and thermal drift. The entire system was kept in a sound proof room and all electronics (computers, controllers, pumps) are kept outside the room where the user can perform the measurements. With all these

precautions in place we achieved a noise level of 0.06 nm (RMS). Images were acquired at 0.5 Hz in tapping mode in order to minimize the forces acting on the sample and also to increase resolution. Adjusting the force curve appropriately minimized the tip-sample contact force, which was determined to be below 5 nN.

3. Results

3.1. Protein to lipid ratio decreased in white ghost preparation

White ghosts were prepared by deliberate extraction of cytoskeletal proteins, while pink ghosts were prepared with maximum preservation of the cytoskeletal proteins. The extent of protein extraction was assessed by measuring the protein to lipid ratio (Fig. 2). The lipid extraction yield was similar for white and pink ghosts. If cytoskeletal proteins were extracted in the white ghosts, a decreased protein to lipid ratio should result. The protein to lipid ratio of white ghosts was determined to be approximately 30% less than the protein to lipid ratio of pink ghosts. Thus, white ghosts contained less cytoskeletal protein than the equivalent pink ghost did. The proportion of each cytoskeletal protein remained essentially the same after extraction, as measured in a SDS-PAGE stained with Coomassie Blue (data not shown). Thus, the findings presented here reflect changes due to the overall loss of cytoskeleton. In order to assess the physical changes that occurred with the extraction of cytoskeleton proteins, the inner surface of white and pink ghosts were imaged using AFM.

3.2. Submembrane cytoskeleton altered by white ghost preparation

The inner submembrane surface topography of white and pink ghosts was imaged with AFM; two representative images are presented (Fig. 3a and b, respectively). Atomic

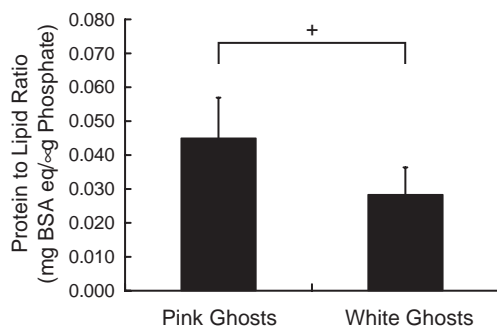


Fig. 2. The extent of cytoskeleton protein loss was determined by measuring the protein to lipid ratio of white and pink ghosts. Complete extraction of intracellular Hb also resulted in a loss of intracellular cytoskeleton proteins. White ghosts contained approximately 30% less cytoskeleton protein content than pink ghosts.

force microscopy directly images the surface topography by measuring the force of attraction/repulsion from the tip of a cantilever with the sample. Thus, an image of the topography of the inner membrane can be generated by scanning over the inner membrane surface. Ghosts were placed on mica slides and lysed. Line traces were made of the white and pink ghost surface to represent the surface topography (Fig. 3c and d, respectively). Pink ghosts exhibited greater variation in surface topography compared to white ghosts. This variation in topography may result from submembrane skeletal proteins or proteins that associate with the submembrane cytoskeleton, such as metHb [25]. The average thickness of white ghosts (14.1 ± 4.0 nm) was less than that of the pink ghosts (18.2 ± 4.5), as reflected in the distribution of thicknesses (Fig. 3e). The average peak to peak distance for white ghosts was 173.4 ± 53.1 nm and was 130.8 ± 45.5 nm for pink ghosts (Fig. 3f). The smaller thickness (Fig. 3e) and the larger peak to peak distance for white ghosts may reflect the depletion of submembrane cytoskeleton and the dissociation of proteins bound to the submembrane cytoskeleton during the washing process to create white ghosts.

3.3. Nitric oxide consumption increased by cytoskeleton extraction

The NO consumption rate of resealed white ghosts was measured using the competition assay [18,22]. By measuring the formation of metHb in the extracellular space of a resealed ghost suspension (15% Hct) containing 10 μ M extracellular oxyHb and 15 μ M Sp/NO and comparing that with the total amount of NO released by Sp/NO, the rate the ghosts consume NO was calculated [19]. No export of oxidizing or reducing species was measured, as described in Materials and methods. Data from resealed ghosts with severe lysis (>5 μ M total Hb released into the extracellular space) were not included in the analysis. The NO uptake rate of resealed white ghosts containing 500 or 1000 μ M oxyHb was 70% and 100% higher than the unmodified RBC (20 mM intracellular Hb) rate of NO uptake, respectively (Fig. 4), on a per RBC basis (k'_{RBC}). As previously reported by Huang et al. [19], when the intracellular Hb decreased below 250 μ M, the NO consumption rate was limited by intracellular Hb.

For controls, pink ghosts in which intracellular Hb was incompletely extracted were tested. Pink ghosts were prepared by lysis of RBCs at ratios empirically determined to result in the desired intracellular Hb concentration. Incomplete extraction of Hb preserved the submembrane cytoskeleton [26], and as a result, the rate of NO uptake of these pink ghosts did not increase as much (Fig. 4). Hence, the observed increase in NO uptake was possibly due to the difference in the submembrane cytoskeleton of resealed white and pink ghosts.

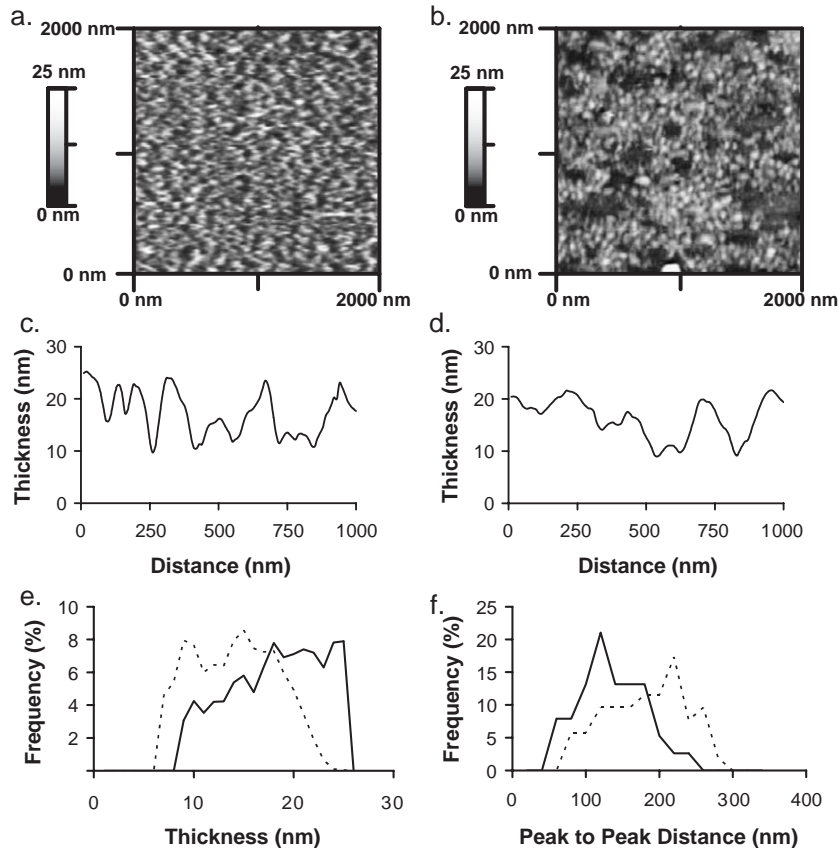


Fig. 3. Atomic force microscopy was used to image the topography of open (a) pink and (b) white ghosts. Constructing a plot from the AFM image along a line, (c) pink ghosts were observed to possess flatter and less frequent peaks compared to (d) white ghosts. (e) The histogram (10 nm bin size) of the pink (solid line) and white (dashed line) ghost submembrane cytoskeleton thickness shows that white ghosts are thinner with an average thickness of 14.1 ± 4.0 nm compared to pink ghosts (18.2 ± 4.5 nm). (f) In addition, the distance from peak to peak (20 nm bin size) was greater for white ghosts (173.4 ± 53.1 nm) than for pink ghosts (130.8 ± 45.5 nm). The valleys between these peaks may represent binding sites for proteins, such as metHb.

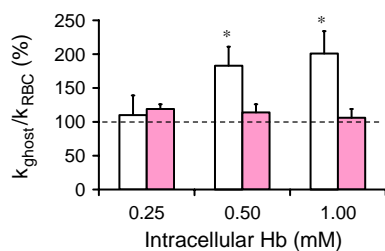


Fig. 4. The NO uptake rate of resealed white (open bars) and pink ghosts (shaded bars) was measured with the competition assay. Compared to the NO uptake rate of unmodified RBCs (20 mM intracellular Hb, dashed horizontal line), resealed white ghosts consumed NO more rapidly at intracellular Hb concentrations of 0.50 (60% higher rate) and 1.00 mM (90% higher rate) (open bars, $*P < 0.05$, $n = 4$ for each concentration). At 0.25 mM intracellular Hb concentration, resealed white ghosts consumption of NO did not statistically differ from that of unmodified RBCs ($n = 4$ for each concentration). This may be due to limitations imposed by the low intracellular Hb concentrations [19,20]. The NO uptake rate of resealed pink ghosts also did not statistically differ from that of unmodified RBCs at all intracellular Hb concentration investigated (shaded bars, $n = 3$ for each concentration). The difference in the NO uptake rate of resealed white and resealed pink ghosts stems from the process of preparation. White ghosts were first extracted of all intracellular Hb and presumably some cytoskeletal proteins which led to the observed increased NO uptake.

4. Discussion

The preservation of NO bioactivity in the presence of Hb-rich blood can be justified by the enclosure of Hb into RBCs. The nature by which NO is preserved from intracellular Hb is complex, but can be separated into four distinct barriers [18]: (i) the creation of an RBC-free zone adjacent to the vessel wall from hydrodynamic forces [15], (ii) high extracellular diffusional resistance from the fluid bulk to the surface of the RBC [16], and (iii) the presence of an intrinsic barrier composed of the RBC submembrane cytoskeletal protein that reduces the entry of NO into the RBC [18,19]. Among the barriers to NO transport, only the RBC intrinsic barrier is present at all times and can be altered to modulate NO bioavailability [18]. Huang et al. proposed that the submembrane cytoskeleton and other relatively NO inert proteins are vital components of this intrinsic barrier using modifications that crosslinked proteins, oxidized hemoglobin, or displaced hemoglobin from the submembrane cytoskeleton [19]. These modifications were hypothesized to lead to physical changes in the underlying submembrane protein structure, as illustrated in

Fig. 5. Han et al. demonstrated that treatment of hypoxic RBCs with nitric oxide accelerated the rate of nitric oxide consumption [20]. Here, we have substantiated the hypothesis of submembrane cytoskeleton resistance to NO transport by demonstrating that physical reduction of the submembrane cytoskeleton leads to an increase in the rate of NO consumption.

The RBC submembrane cytoskeleton has been estimated to range from 18 to 60 nm in thickness in its native state [27,28]. As shown here and in other studies, the RBC submembrane cytoskeleton possesses a complex three dimensional structure [29], which may force NO and other small molecules to traverse tortuous channels or pores to access intracellular Hb. Prior studies that address the structure of the submembrane cytoskeleton failed to image the cytoskeleton in its native state [30–33]. In those studies, the submembrane cytoskeleton was artificially stretched in order to obtain an image of a two-dimensional mesh-like network of spectrin fibers. Hence, these extrapolations on the role of the cytoskeleton in the uptake of NO do not consider that the native state cytoskeleton is more dense and compressed than the stretched cytoskeleton [34].

Previously, questions regarding the role of the submembrane cytoskeleton as a barrier to NO entry into RBCs have been put forth by Liu et al. [34]. This discussion revolves around a mathematical analysis of the competition assay. Following the prior O₂ transport literature, Liu et al. suggested that an unstirred layer surrounding each RBC is

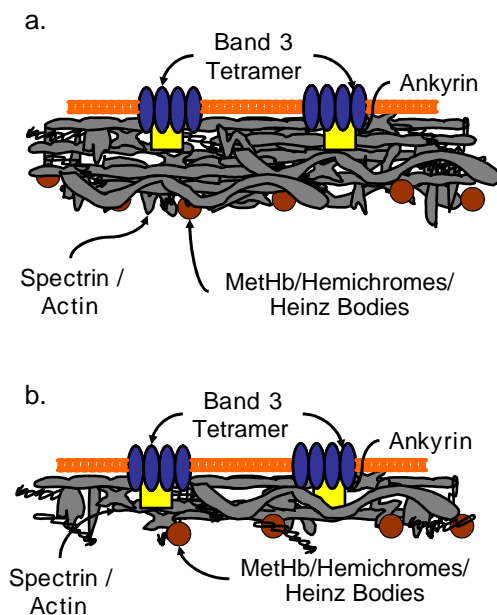


Fig. 5. The entry of NO into the RBC is reduced by the submembrane cytoskeleton. Other relatively NO inert proteins, such as metHb, hemichromes, and Heinz bodies, also contribute to the reduction in NO entry. (a) Unmodified RBCs or pink ghosts possess a submembrane cytoskeleton that effectively reduces the rate of NO entry. The submembrane cytoskeleton is bound to the submembrane through the ankyrin/Band 3 association. (b) Reduction of the submembrane cytoskeleton by forming resealed white ghosts leads to an increase in the rate of NO entry.

the primary component responsible for the preservation of NO bioactivity [16,34]. However, if an external, unstirred layer was the primary mode by which NO is preserved, then chemical modifications using Band 3 crosslinkers, sodium azide, phenylhydrazine, or nitric oxide, itself, [19,20] or submembrane cytoskeleton depletion, as shown in this study, should have no impact on the rate of NO consumption by RBCs. As these modifications did not significantly change the RBC morphology, the alteration of an intrinsic barrier is the most likely explanation for the observed changes in the NO uptake rate. Moreover, recent simulations on the reaction and diffusion of endothelium derived NO have reinforced the finding that the RBC must possess an intrinsic barrier to NO diffusion [20,35]. Prior studies that investigated the kinetics of NO uptake by RBCs were limited by extremely low hematocrits (0.01%–0.15%), which may have inflated the importance of external diffusion [36]. The experiments performed here and in our prior studies were performed at hematocrits (15%–20%) that better reflect those found in vivo (~40%–45%). In addition, the use of a slow releasing NO donor at these hematocrits diminishes external barriers to NO [18,22]. This allowed for the determination of whether intrinsic factors were responsible for the low rate of NO uptake. It is likely that under certain conditions, the external barrier is important; however, the intrinsic barrier is always present.

The submembrane cytoskeleton barrier has the vital function of reducing the rate that NO is metabolized in the vasculature [18]. Endothelium derived NO can diffuse to adjacent smooth muscle cells to activate soluble guanylyl cyclase, which initiates a cascade of interactions that leads to vasodilation. In addition to preserving endothelium derived NO, the submembrane cytoskeleton barrier may also play a role in the delivery of NO from the RBC. Recent studies have identified deoxyHb as a mediator in the formation of NO bioactivity [23,37,38]. Once formed, NO either binds deoxyHb, reacts with oxyHb, or escapes into the plasma. The reuptake of NO that escapes into the plasma is effectively slowed by the submembrane cytoskeleton barrier. In turn, this allows NO to diffuse to the smooth muscle cell to initiate the cascade of interactions that results in vasodilation.

Since the specific extraction of submembrane cytoskeletal proteins could not be achieved, our conclusion at this point is that the submembrane cytoskeletal proteins reduce NO entry into the RBC by physically retarding NO diffusion. With further studies using RBCs from knockout mice or other animal strains, the specific protein or set of proteins may be identified. The extraction of the submembrane cytoskeletal proteins resulted in an increase in the rate of NO entry. Whether this preparation also increases the rate of entry for other small gas molecules, such as dioxygen and carbon monoxide, is an interesting topic that needs further study.

We have recently demonstrated that exposure of hypoxic RBCs to NO to form iron-nitrosylhemoglobin results in an

increase in the rate RBCs consume NO [20]. Therefore, it appears that NO consumption by RBC can be regulated under physiological or pathophysiological conditions. The results presented here strengthen the hypothesis that NO consumption rate by RBC is limited by an RBC intrinsic barrier (which can be modulated), rather than an extrinsic diffusion layer which cannot be regulated. An intrinsic barrier that can modulate the entry of NO may have physiological and therapeutic relevance. The regulation of NO consumption was suggested to occur under conditions such as hypoxic pulmonary vasoconstriction, ischemic vasospasm, and inhaled NO therapy. In addition, as the submembrane cytoskeleton is the primary barrier within the RBC to NO entry, blood substitutes that do not incorporate a barrier to NO entry may have difficulties emulating the NO preserving properties of RBCs.

Acknowledgements

This work was funded by NIH grant R01 HL65741. THH was supported, in part, by the NIH National Research Service Award T32 HL07895 from the National Heart, Lung, and Blood Institute. The authors would like to acknowledge technical assistance from Andrew E. Pelling and James K. Gimzewski in acquiring AFM images, Tae-joon Jeon for preparing ghosts for AFM measurements, and Alan S. Sohn for measuring the protein to lipid ratios.

References

- [1] W.P. Arnold, C.K. Mittal, S. Katsuki, F. Murad, Nitric oxide activates guanylate cyclase and increases guanosine 3':5'-cyclic monophosphate levels in various tissue preparations, *Proc. Natl. Acad. Sci. U. S. A.* 74 (1977) 3203–3207.
- [2] R.F. Furchgott, J.V. Zawadzki, The obligatory role of endothelial cells in the relaxation of arterial smooth muscle by acetylcholine, *Nature* 288 (1980) 373–376.
- [3] L.J. Ignarro, G.M. Buga, K.S. Wood, R.E. Byrns, G. Chaudhuri, Endothelium-derived relaxing factor produced and released from artery and vein is nitric oxide, *Proc. Natl. Acad. Sci. U. S. A.* 84 (1987) 9265–9269.
- [4] R.M. Palmer, A.G. Ferrige, S. Moncada, Nitric oxide release accounts for the biological activity of endothelium-derived relaxing factor, *Nature* 327 (1987) 524–526.
- [5] M.P. Doyle, J.W. Hoekstra, Oxidation of nitrogen oxides by bound dioxygen in hemoproteins, *J. Inorg. Biochem.* 14 (1981) 351–358.
- [6] S. Herold, M. Exner, T. Nausser, Kinetic and mechanistic studies of the NO*-mediated oxidation of oxymyoglobin and oxyhemoglobin, *Biochemistry* 40 (2001) 3385–3395.
- [7] T.H. Han, J.M. Fukuto, J.C. Liao, Reductive nitrosylation and S-nitrosation of hemoglobin in inhomogeneous nitric oxide solutions, *Nitric Oxide* 10 (2004) 74–82.
- [8] J.R. Lancaster Jr., Simulation of the diffusion and reaction of endogenously produced nitric oxide, *Proc. Natl. Acad. Sci. U. S. A.* 91 (1994) 8137–8141.
- [9] D.H. Doherty, M.P. Doyle, S.R. Curry, R.J. Vali, T.J. Fattor, J.S. Olson, D.D. Lemon, Rate of reaction with nitric oxide determines the hypertensive effect of cell-free hemoglobin, *Nat. Biotechnol.* 16 (1998) 672–676.
- [10] Z. Huang, J.G. Louderback, M. Goyal, F. Azizi, S.B. King, D.B. Kim-Shapiro, Nitric oxide binding to oxygenated hemoglobin under physiological conditions, *Biochim. Biophys. Acta* 1568 (2001) 252–260.
- [11] T.H. Han, D.R. Hyduke, M.W. Vaughn, J.M. Fukuto, J.C. Liao, Nitric oxide reaction with red blood cells and hemoglobin under heterogeneous conditions, *Proc. Natl. Acad. Sci. U. S. A.* 99 (2002) 7763–7768.
- [12] C.D. Reiter, X. Wang, J.E. Tanus-Santos, N. Hogg, R.O. Cannon III, A.N. Schechter, M.T. Gladwin, Cell-free hemoglobin limits nitric oxide bioavailability in sickle-cell disease, *Nat. Med.* 8 (2002) 1383–1389.
- [13] L. Jia, C. Bonaventura, J. Bonaventura, J.S. Stamler, S-nitrosohaemoglobin: a dynamic activity of blood involved in vascular control, *Nature* 380 (1996) 221–226.
- [14] M.W. Vaughn, L. Kuo, J.C. Liao, Effective diffusion distance of nitric oxide in the microcirculation, *Am. J. Physiol.* 274 (1998) H1705–H1714.
- [15] J.C. Liao, T.W. Hein, M.W. Vaughn, K.T. Huang, L. Kuo, Intravascular flow decreases erythrocyte consumption of nitric oxide, *Proc. Natl. Acad. Sci. U. S. A.* 96 (1999) 8757–8761.
- [16] X. Liu, M.J. Miller, M.S. Joshi, H. Sadowska-Krowicka, D.A. Clark, J.R. Lancaster Jr., Diffusion-limited reaction of free nitric oxide with erythrocytes, *J. Biol. Chem.* 273 (1998) 18709–18713.
- [17] J.S. Olson, E.W. Foley, C. Rogge, A.L. Tsai, M.P. Doyle, D.D. Lemon, No scavenging and the hypertensive effect of hemoglobin-based blood substitutes, *Free Radic. Biol. Med.* 36 (2004) 685–697.
- [18] M.W. Vaughn, K.T. Huang, L. Kuo, J.C. Liao, Erythrocytes possess an intrinsic barrier to nitric oxide consumption, *J. Biol. Chem.* 275 (2000) 2342–2348.
- [19] K.T. Huang, T.H. Han, D.R. Hyduke, M.W. Vaughn, H. Van Herle, T.W. Hein, C. Zhang, L. Kuo, J.C. Liao, Modulation of nitric oxide bioavailability by erythrocytes, *Proc. Natl. Acad. Sci. U. S. A.* 98 (2001) 11771–11776.
- [20] T.H. Han, E. Qamirani, A.G. Nelson, D.R. Hyduke, G. Chaudhuri, L. Kuo, J.C. Liao, Regulation of nitric oxide consumption by hypoxic red Blood Cells, *Proc. Natl. Acad. Sci. U. S. A.* 100 (2003) 12504–12509.
- [21] T.L. Steck, J.A. Kant, Preparation of impermeable ghosts and inside-out vesicles from human erythrocyte membranes, *Methods Enzymol.* 31 (1974) 172–180.
- [22] M.W. Vaughn, K.T. Huang, L. Kuo, J.C. Liao, Erythrocyte consumption of nitric oxide: competition experiment and model analysis, *Nitric Oxide* 5 (2001) 18–31.
- [23] K. Cosby, K.S. Partovi, J.H. Crawford, R.P. Patel, C.D. Reiter, S. Martyr, B.K. Yang, M.A. Waclawiw, G. Zalos, X. Xu, K.T. Huang, H. Shields, D.B. Kim-Shapiro, A.N. Schechter, R.O. Cannon III, M.T. Gladwin, Nitrite reduction to nitric oxide by deoxyhemoglobin vasodilates the human circulation, *Nat. Med.* 9 (2003) 1498–1505.
- [24] X. Zhou, G. Arthur, Improved procedures for the determination of lipid phosphorus by malachite green, *J. Lipid Res.* 33 (1992) 1233–1236.
- [25] B. Giardina, R. Scatena, M.E. Clementi, M.T. Ramacci, F. Maccari, L. Cerroni, S.G. Condo, Selective binding of met-hemoglobin to erythrocytic membrane: a possible involvement in red blood cell aging, *Adv. Exp. Med. Biol.* 307 (1991) 75–84.
- [26] T.L. Steck, in: W.D. Stein, F. Bronner (Eds.), *Cell Shape: Determinants, Regulation, and Regulatory Role*, Academic Press, New York, 1989, pp. 205–246.
- [27] V. Heinrich, K. Ritchie, N. Mohandas, E. Evans, Elastic thickness compressibility of the red cell membrane, *Biophys. J.* 81 (2001) 1452–1463.
- [28] B.S. Bull, R.S. Weinstein, R.A. Korpman, On the thickness of the red cell membrane skeleton: quantitative electron microscopy of maximally narrowed isthmus regions of intact cells, *Blood Cells* 12 (1986) 25–42.

- [29] A.H. Swihart, J.M. Mikrut, J.B. Ketterson, R.C. Macdonald, Atomic force microscopy of the erythrocyte membrane skeleton, *J. Microsc.* 204 (2001) 212–225.
- [30] A.M. McGough, R. Josephs, On the structure of erythrocyte spectrin in partially expanded membrane skeletons, *Proc. Natl. Acad. Sci. U. S. A.* 87 (1990) 5208–5212.
- [31] S.C. Liu, L.H. Derick, J. Palek, Visualization of the hexagonal lattice in the erythrocyte membrane skeleton, *J. Cell Biol.* 104 (1987) 527–536.
- [32] B.W. Shen, R. Josephs, T.L. Steck, Ultrastructure of the intact skeleton of the human erythrocyte membrane, *J. Cell Biol.* 102 (1986) 997–1006.
- [33] T.J. Byers, D. Branton, Visualization of the protein associations in the erythrocyte membrane skeleton, *Proc. Natl. Acad. Sci. U. S. A.* 82 (1985) 6153–6157.
- [34] X. Liu, A. Samouilov, J.R. Lancaster Jr., J.L. Zweier, Nitric oxide uptake by erythrocytes is primarily limited by extracellular diffusion not membrane resistance, *J. Biol. Chem.* 277 (2002) 26194–26199.
- [35] N.H. El-Farra, P.D. Christofides, J.C. Liao, Analysis of nitric oxide consumption by erythrocytes in blood vessels using a distributed multicellular model, *Ann. Biomed. Eng.* 31 (2003) 294–309.
- [36] J.C. Merchuk, Z. Tzur, E.N. Lightfoot, Diffusional resistances to oxygen transfer in whole blood, *Chem. Eng. Sci.* 38 (1983) 1315–1321.
- [37] C.J. Hunter, A. Dejam, A.B. Blood, H. Shields, D.B. Kim-Shapiro, R.F. Machado, S. Tarekegn, N. Mulla, A.O. Hopper, A.N. Schechter, G.G. Power, M.T. Gladwin, Inhaled nebulized nitrite is a hypoxia-sensitive NO-dependent selective pulmonary vasodilator, *Nat. Med.* 10 (2004) 1122–1127.
- [38] D.B. Kim-Shapiro, M.T. Gladwin, R.P. Patel, N. Hogg, The reaction between nitrite and hemoglobin: the role of nitrite in hemoglobin-mediated hypoxic vasodilation, *J. Inorg. Biochem.* 99 (2005) 237–246.